A β-galactosidase-activated luminogen with aggregation-induced emission feature for cancer senescence imaging and monitoring in vivo

Peili Cen, Mei Tian, Hong Zhang

Zhejiang University School of Medicine, Hangzhou, 310009, Zhejiang, China.

Introduction

- Cellular senescence is a permanent state of cell cycle arrest characterized by increased activity of senescence associated β-galactosidase (SA-β-gal).
- Cancer cells can also enter a senescent state induced by anticancer therapies and be considered for sequential treatment with pro-senescence followed by senolysis.
- However, there is currently no effective imaging agent targeting β-galactosidase (β-Gal) for imaging and monitoring senescent cancer cells in vivo.
- Aggregation-induced emission luminogen (AIEgen) demonstrates strong fluorescence, good photostability, and biocompatibility, making it a potential candidate for imaging and monitoring senescent cancer cells in vivo when endowed with β-Gal-responsive capabilities.
- This study aims to report a β-Gal-activated AIEgen called QM-β-gal for cancer senescence imaging and senolysis monitoring in vivo.

Methods

- QM-β-gal was synthesized and characterized. The absorption and emission spectra, specific enzyme responses were analyzed before and after activation by β-Gal.
- MDA-MB-231 tumor-bearing mouse model was induced into cancer senescence by doxorubicin (DOX) and injected with QM-β-gal through tail vein to image senescent cancer cells in vivo.
- Mice were sacrificed to collect serum, tumor, liver and kidney at various time points to quantify circulation half-time and metabolism of QM-β-gal.
- Blood serum biochemical tests and major organs HE staining were implemented to evaluate biosafety in vivo.
- To monitor the senolysis, QM-β-gal was injected to monitor the process of senolysis induced by ABT263 on DOX-induced senescent tumor in vivo.

Structure and characteristics of QM-β-gal

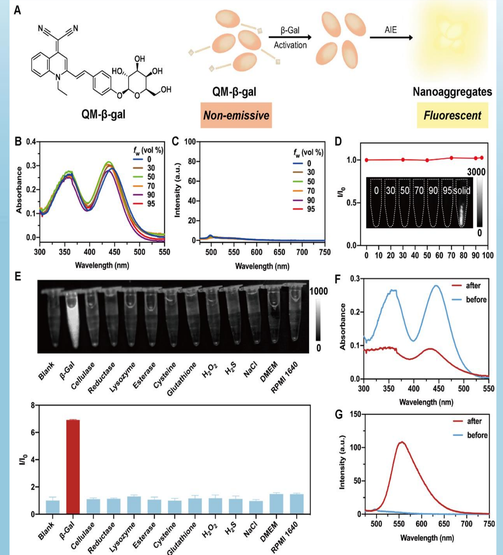

Figure 1. A) Chemical structure of QM-β-gal and illustrated process of activation by β-Gal; B) Absorption spectra of QM-β-gal (10μM) with different water fractions (f_w) in a mixture of water/DMSO; C) Emission spectra of QM-β-gal (10μM) with different f_w; D) I/I_0 plots and fluorescent images of QM-β-gal (10μM) and solid state in different f_w, where I is the fluorescence intensity collected at 572nm and I_0 is the fluorescence intensity of QM-β-gal in 0% water, λ_{ex}=437nm; E) Fluorescence response at 572nm of QM-β-gal (10μM) incubated with β-Gal (6U) in aqueous solution (50mM, pH=7.4) at 37℃ and other components containing cellulase, reductase, lysozyme, esterase, cysteine, glutathione, H_2O_2, H_2S, NaCl, and different culture mediums in the same condition, λ_{ex}=437nm; F) Absorption spectra of QM-β-gal (10μM) before and after activation by β-Gal; G) Emission spectra of QM-β-gal (10μM) before and after activation by β-Gal.

In vivo behaviors of QM-β-gal in DOX-induced senescent tumor-bearing mice

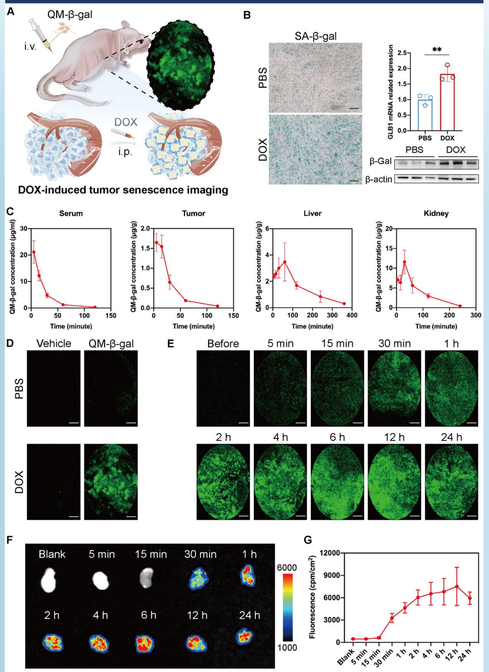

Figure 2. A) Illustration of DOX-induced cancer senescence and fluorescence imaging by injection of QM-β-gal through tail vein on MDA-MB-231 tumor-bearing nude mice; B) SA-β-gal staining of tumor slices, and GLB1 mRNA and β-Gal expression of tumor tissues between PBS and DOX groups; C) The concentrations of QM-β-gal at different time points in the serum, tumor, liver, and spleen of DOX group; D) In vivo optical fiber confocal imaging in the tumors of PBS and DOX groups with/without QM-β-gal injection; E) In vivo optical fiber confocal imaging at different time points in the tumor of DOX group; F) and G) Ex vivo fluorescence imaging and quantitative analysis at time points on tumors.

Long-term fluorescence imaging of DOX-induced cancer senescence in vivo

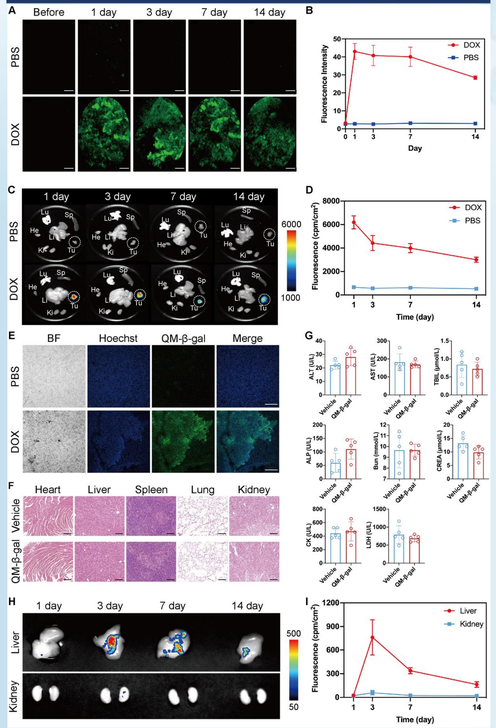

Figure 3. A) and B) In vivo optical fiber confocal fluorescence imaging and fluorescence intensity of tumors before and after; C) Ex vivo fluorescence imaging of tumors and major organs after QM-β-gal injection; D) Ex vivo fluorescence intensity of tumors before and after QM-β-gal injection; E) Confocal fluorescence imaging of ex vivo tumor slices with QM-β-gal and Hoechst after 14 days post injection; F) HE staining after 14 days post QM-β-gal or vehicle injection; G) Serum biochemical indexes; H) and I) Ex vivo fluorescence imaging and quantitative analysis of liver and kidney after QM-β-gal injection in DOX group.

In vivo senolysis monitoring of ABT263 treatment by QM-β-gal after pro-senescence

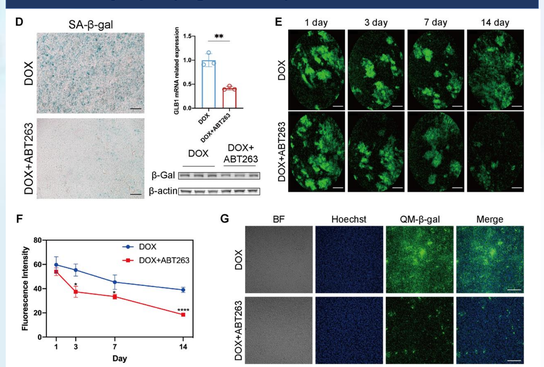

Figure 4. D) SA-β-gal staining of tumor slices and expressions of mRNA and β-Gal in DOX and DOX+ABT263 groups; E) and F) In vivo optical fiber confocal fluorescence imaging and fluorescence intensity; G) Fluorescence imaging of tumor slices with QM-β-gal and Hoechst.

Conclusions

- QM-β-gal could image and monitor senescent cancer cells during pro-senescence therapy with DOX followed by senolysis with ABT263 in vivo.
- It exhibited rapid clearance but stable retention over time after activation within DOX-induced senescent tumors and demonstrated long-term imaging capabilities for senescent cancer cells lasting over 14 days throughout the sequential treatment process.
- QM-β-gal had the potential to be a promising candidate for labeling senescent cells with high specificity and stability for fluorescence imaging in vivo.

Contact

Prof. Hong Zhang: hzhang21@zju.edu.cn